

This article was downloaded by: [Purdue University]

On: 05 March 2013, At: 01:40

Publisher: Taylor & Francis

Informa Ltd Registered in England and Wales Registered Number: 1072954

Registered office: Mortimer House, 37-41 Mortimer Street, London W1T 3JH, UK



## International Journal of Polymeric Materials and Polymeric Biomaterials

Publication details, including instructions for authors and subscription information:

<http://www.tandfonline.com/loi/gpom20>

### Nematic Electroclinic Effect in Mixtures

Joseba Zubia<sup>a</sup> & Jesus Etxebarria Ecenarro<sup>b</sup>

<sup>a</sup> Depto. de Automatica, Electronicay Telecomunicaciones, ETSIIT, Universidad del Pais Vasco Alameda de Urquijo s/n, 48013, Bilbao, Spain

<sup>b</sup> Depto. de Fisica de la Materia Condensada, Universidad del Pais Vasco, Apto. 644, 48080, Bilbao, Spain

Version of record first published: 27 Oct 2006.

To cite this article: Joseba Zubia & Jesus Etxebarria Ecenarro (2000): Nematic Electroclinic Effect in Mixtures, International Journal of Polymeric Materials and Polymeric Biomaterials, 45:3-4, 503-532

To link to this article: <http://dx.doi.org/10.1080/00914030008035052>

PLEASE SCROLL DOWN FOR ARTICLE

Full terms and conditions of use: <http://www.tandfonline.com/page/terms-and-conditions>

This article may be used for research, teaching, and private study purposes. Any substantial or systematic reproduction, redistribution, reselling, loan, sub-licensing, systematic supply, or distribution in any form to anyone is expressly forbidden.

The publisher does not give any warranty express or implied or make any representation that the contents will be complete or accurate or up to date. The accuracy of any instructions, formulae, and drug doses should be

independently verified with primary sources. The publisher shall not be liable for any loss, actions, claims, proceedings, demand, or costs or damages whatsoever or howsoever caused arising directly or indirectly in connection with or arising out of the use of this material.

# Nematic Electroclinic Effect in Mixtures

JOSEBA ZUBIA<sup>a,\*</sup> and JESUS ETXEBARRIA ECENARRO<sup>b</sup>

<sup>a</sup> *Depto. de Automatica, Electronica y Telecomunicaciones, ETSIIT, Universidad del Pais Vasco Alameda de Urquijo s/n, 48013 Bilbao, Spain;*

<sup>b</sup> *Depto. de Fisica de la Materia Condensada, Universidad del Pais Vasco, Apto. 644, 48080 Bilbao, Spain*

*(Received 18 December 1998)*

Origin of the nematic electroclinic effect (NEE) in monomer liquid crystals (MLCs) and in polymer liquid crystals (PLCs) is discussed. Results for two different compounds, one forming a smectic A and another forming a smectic C phase are reported, along with results for the mixtures of these two compounds. Different explanations of NEE are analyzed on the basis of the experimental results and the most plausible explanation is pointed out.

*Keywords:* Nematic electroclinic effect (NEE); monomer liquid crystals (MLCs); polymer liquid crystals (PLCs); smectic A phase; smectic C phase

## 1. INTRODUCTION

The electroclinic effect (from now on EE) was first described by Garoff and Meyer [1] two years after the discovery of ferroelectricity in liquid crystals [2]. By means of a symmetry argument similar to that predicting ferroelectricity in a chiral smectic C ( $S_C$ ), these authors described the origin of the EE in a smectic A mesophase ( $S_A$ ), composed of chiral molecules. When an electric field is applied to a chiral non tilted smectic liquid crystal, an inclination of the molecules in the plane normal to the electric field is induced. Thus, the  $S_A$  phase can be considered as a retardation plate with a field sensitive optic axis. This property is commonly used in devices for fast light intensity modulation.

---

\*Corresponding author.

During the subsequent years large amounts of effort were dedicated to the study of this effect due to its considerable interest, not only from a fundamental but also from a practical point of view [3–11]. However, most of this work was focused on the study of the behaviour of the EE in orthogonal smectic phases.

The electroclinic effect has been observed in monomer as well as in polymer liquid crystals (PLCs) [12–16]. Although the molecular motion seems to be more complicated in the case of PLCs, the magnitude of the induced tilt angle in the  $S_A$  phase is similar for polymers and for low molecular weight mesogens. One way to characterize the strength of the effect similarity is through the coupling constant  $C_1 = P/\theta$ , which is the ratio between the induced polarization and the induced tilt angle. Typical values of this parameter lay in the range of 300–500 nC/cm<sup>2</sup>rad for both, MLC and PLC materials [4, 12].

Komitov [17] and Li [18] have shown independently that the presence of smectic layers is not essential for the appearance of an optical tilt proportional to the applied field. In the chiral nematic phase ( $N$ ) of a material with a long pitch, a tilt of the optical tensor proportional to the amplitude of the electric field can be obtained if the cholesteric helix is unwound by means of surface stabilization. This electroclinic response has been found to be of relatively small amplitude and, up to now, no successful attempt has been made to fit the critical behaviour of this effect in the  $N-S_A$  transition [18–21].

We will begin by presenting the basic principles of the EE in orthogonal smectics. Then we will review the main theories that have appeared in the literature in order to explain the origin of the electroclinic effect in nematics (NEE). A simple model for some dynamical aspects of the NEE will be also given. Next section will deal with the measurement system. The experimental procedure is described with some detail and some inherent problems associated to the measurement process will be pointed out.

Section 3 is dedicated to present some examples of typical NEE results. The experimental data of two different compounds with  $N-S_A$  and  $N-S_C$  phase transitions respectively are shown together with data corresponding to several mixtures made from them. Some results on the dynamics of the NEE are also shown in this section.

In the final part of the paper we will discuss the different explanations that have been suggested to explain the nature of NEE, its

dynamics and its critical behaviour around the  $N-S_A$  phase transition. As a conclusion we will point out the most plausible nature of the phenomenon.

## 2. ORIGIN OF THE NEMATIC ELECTROCLINIC EFFECT

Before analysing the NEE, we will first consider the basis for the EE in smectics, which is a kind of inverse piezoelectric effect. A symmetry argument can be used to explain the appearance of the effect [22]. In the  $S_A$  phase, the long molecular axes are arranged parallel to each other in average and the molecular director  $\mathbf{n}$  is parallel to the smectic layer normal. The molecules, as follows from high frequency dielectric measurements, are free to rotate around their long axes [23]. If an electric field  $\mathbf{E}$  is applied parallel to the smectic layers, the free rotation is hindered due to the coupling of the electric field with the transverse component of the molecular dipole moment  $\mathbf{p}$ . In this situation and assuming the head to tail equivalence of the molecular director  $\mathbf{n} \rightarrow -\mathbf{n}$ , the direction of the electric field  $\mathbf{E}$  is a twofold axis of the system. If the molecules are non chiral, the plane containing  $\mathbf{n}$  and  $\mathbf{p}$  is a symmetry plane. On the contrary, if the molecules are chiral this symmetry does not exist any more. Therefore, the free energy is not a symmetric function of the tilt angle and the molecular director  $\mathbf{n}$  will deviate from the layer normal direction to its new tilted position. Tilt angles as large as of  $20^\circ$  for electric fields  $E = 20 \text{ V}/\mu\text{m}$  have been reported [24]. This argument is exposed graphically in Figure 1.

In the following we will review some of the theoretical treatments that have appeared in the literature to explain the NEE. At this stage, theories will be presented without discussion. The first two theories consider the NEE as a bulk process and the last one as a surface effect. The reliability of these arguments will be discussed later on.

### 2.1. Molecular Origin of the Nematic Electroclinic Effect

The symmetry argument predicting the coupling between the tilt angle and the polarization is not restricted to a special kind of smectic phases. The EE is a universal property of both nontilted and tilted smectic phases containing chiral molecules. Other phases and, in

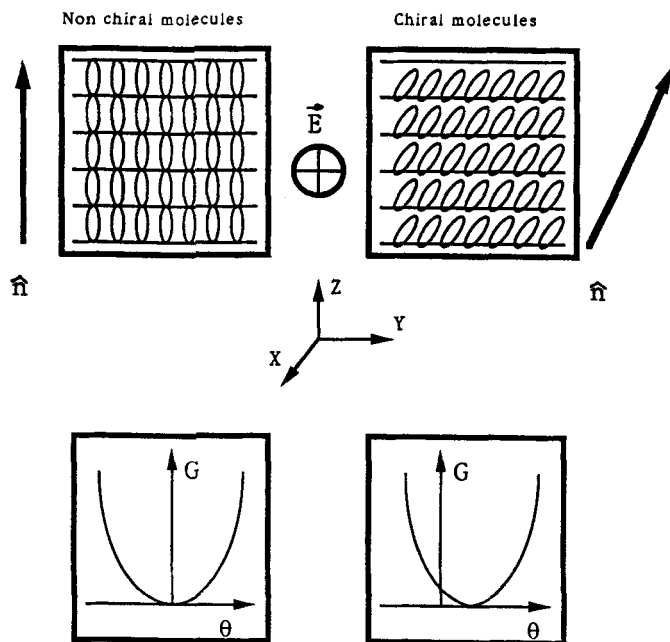


FIGURE 1 Symmetry argument to explain the appearance of the EE in smectic phases. If an electric field is applied parallel to the smectic planes, the molecular dipole moment  $\mathbf{p}$  will be oriented parallel to the field. The direction of the electric field is a twofold axis. The plane containing the nematic director  $\mathbf{n}$  and the dipole moment  $\mathbf{p}$  is a mirror plane if the molecules are non chiral. Otherwise chirality destroys this symmetry. In this case, the free energy  $G$  is no longer a symmetric function of  $\theta$  and a molecular tilt is induced in a plane perpendicular to the  $\mathbf{n}-\mathbf{p}$  plane.

particular, the  $N$  phase, might also be expected to exhibit such an effect [17–18]. A symmetry-based phenomenological model of the NEE has been given in Refs. [18, 19]. Here we will offer a simple argument that easily permits one to intuit the phenomenon on a molecular level [20].

Consider a  $N$  phase which contains molecules of zigzag shape (Fig. 2) in such a way that the description of their orientation requires the use of two unit vectors,  $\mathbf{n}_1$  (the usual nematic director) and  $\mathbf{n}_2$ . In this situation, the optical dielectric tensor  $\epsilon_{ij}$  (or any symmetric second rank tensor) can be expressed to lowest order as:

$$\epsilon_{ij} = \epsilon_0 \delta_{ij} + \epsilon_1 \langle \mathbf{n}_1 \mathbf{n}_1 \rangle + \epsilon_2 \langle \mathbf{n}_1 \mathbf{n}_2 + \mathbf{n}_2 \mathbf{n}_1 \rangle + \epsilon_3 \langle \mathbf{n}_2 \mathbf{n}_2 \rangle \quad (1)$$

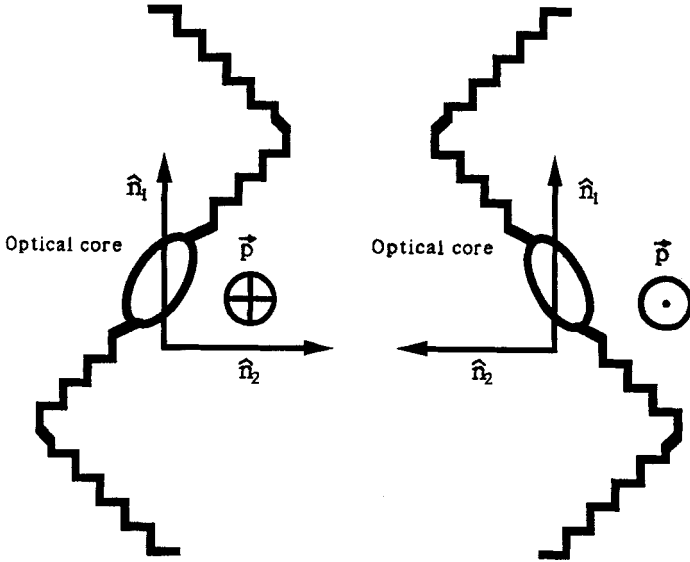


FIGURE 2 Schematic representation of zig-zag shaped molecules. For  $\mathbf{E} = 0$ , both configurations have the same energy. For  $\mathbf{E} \neq 0$  this symmetry is broken and one of the configurations becomes more probable. Then, the optical tensor will not be codiagonal with the inertial tensor any more.  $\mathbf{n}_1$  is the usual nematic director and  $\mathbf{n}_2$  is a second nematic director perpendicular to  $\mathbf{n}_1$ , which accounts for the orientation of other molecular parts. The molecule is supposed to have a dipole moment given by  $\mathbf{p} = \mu \mathbf{n}_1 \times \mathbf{n}_2$ .

where  $\epsilon_0, \epsilon_1, \epsilon_2$  and  $\epsilon_3$  are constants and the symbol  $\langle \rangle$  denotes thermodynamic average. In order to simplify, let us consider that  $\mathbf{n}_1$  is perfectly oriented (the nematic order parameter is equal to unity) and  $\mathbf{n}_2$  is orthogonal to  $\mathbf{n}_1$  so that  $\mathbf{n}_1 = (0, 0, 1)$  and  $\mathbf{n}_2 = (\cos\varphi, \sin\varphi, 0)$ . The molecules are supposed to have strong lateral dipoles whose value is given by  $\mathbf{p} = \mu \mathbf{n}_1 \times \mathbf{n}_2$ . If we apply an electric field  $\mathbf{E} = (E, 0, 0)$ , the molecules will have an energy  $V = -\mathbf{p} \cdot \mathbf{E} = -\mu E \sin\varphi$  from which the average values of the different trigonometric functions of  $\varphi$  can be calculated. For example,  $\langle \sin\varphi \rangle$  will be given by:

$$\langle \sin\varphi \rangle = \frac{\int_0^{2\pi} \sin\varphi \exp(-V/kT) d\varphi}{\int_0^{2\pi} \exp(-V/kT) d\varphi} = -\mu E / 2kT \quad (2)$$

assuming the inequality  $\mu E \ll kT$ . Using the above expression for  $\varepsilon_{ij}$  we get:

$$\begin{bmatrix} \varepsilon_0 + \varepsilon_3/2 & 0 & 0 \\ 0 & \varepsilon_0 + \varepsilon_3/2 & -\varepsilon_2\mu E/2kT \\ 0 & -\varepsilon_2\mu E/2kT & \varepsilon_0 + \varepsilon_1 \end{bmatrix} \quad (3)$$

Therefore, the presence of the field causes the old principal axes parallel to  $z$  and  $y$  to rotate by an angle  $\theta$  given by  $\tan 2\theta = 2\varepsilon_{32}/(\varepsilon_{33} - \varepsilon_{22})$ , *i.e.*,

$$\theta = \frac{-\varepsilon_2\mu E}{kT(\varepsilon_1 - \varepsilon_2/2)} \quad (4)$$

which it is linear in the electric field.

If the nematic order parameter  $s$  is not completely saturated, the results are qualitatively similar.

## 2.2. Cybotactic Clusters

In the  $N$  phase, just above the transition to a smectic phase, small domains with smectic organization are formed. It was De Vries [25] who first recognized this fact, calling these domains cybotactic clusters (Fig. 3). The coupling between the electric field and the local polarization promotes the molecules and the local optic axis to follow the variations of the electric field, leading to a modulation of the light intensity across the sample. According to Marcerou [26], when an electric field  $\mathbf{E} = (E, 0, 0)$  is applied, a non zero component of the density modulation wave vector  $q_y$ , appears which is proportional to the electric field [ $\mathbf{q} = (0, q_y, q_s)$ ].

$$q_y/q_s = \theta = \varepsilon_0\chi_R CE/\sigma(T - T_{AC}) \quad (5)$$

In this equation  $C$  represents the coefficient associated to the trilinear coupling between the polarization and the density modulations in the direction parallel and normal to the local director,  $\sigma$  is a positive constant and  $q_s = 2\pi/a$  where  $a$  is the layer thickness. The so-called normalized susceptibility  $\chi_R$  increases as we approach the nematic-smectic transition temperature with a critical exponent which



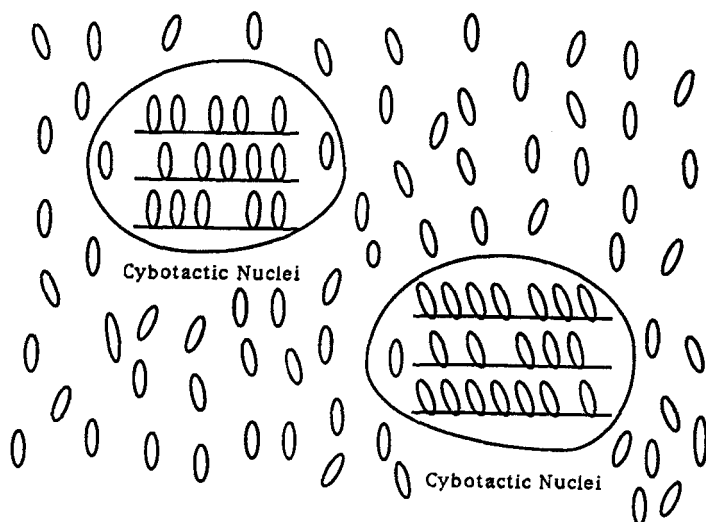


FIGURE 3 Cybotactic groups above a smectic-nematic transition. In the cybotactic nuclei, the molecules are arranged perpendicularly to the smectic layers above a  $N-S_A$  transition and tilted above a  $N-S_C$  transition.

depends on the proximity to the NAC ( $N-S_A-S_C$ ) point, where the susceptibility diverges [26].

### 2.3. Surface Nature of the Nematic Electroclinic Effect

The rubbing direction as a conceptually different axis from the nematic director can also be used to explain the observed effect at the  $N-S_A$  transition. According to Ref. [27], in the  $N$  phase there exists the possibility of surface contributions to the Helmholtz function of chiral nature of the form:

$$\delta A_S = \int dS K_c (\mathbf{s} \cdot \mathbf{n}) [\mathbf{s} \cdot (\mathbf{E} \times \mathbf{n})] \quad (6)$$

where  $\delta A_S$  is the surface Helmholtz function contribution,  $dS$  is the surface element,  $K_c$  a constant dependent on the surface,  $\mathbf{s}$  is a unit vector along the rubbing direction,  $\mathbf{n}$  the molecular director and  $\mathbf{E}$  the electric field.

The above term can be written as:

$$\delta A_S = -SK_c \mathbf{E} \theta(0) \quad (7)$$

for small tilts  $\theta(0)$  of the surface molecules with respect to the rubbing axis. In the absence of field, the surface Helmholtz function takes the form [25]:

$$A_S = 1/2SK_s \theta(0)^2 \quad (8)$$

where  $K_s$  is a positive constant, thus favouring  $\theta(0) = 0$ . It can be easily shown that the additional term  $\delta A_S$  produces a tilt on the surface molecules  $\theta(0) = K_c/K_s \mathbf{E}$ , which is linear in the electric field. The rotation of the alignment at the surface can then give rise to a nonzero tilt value along the whole sample thickness, whose instantaneous deformation profile upon the application of an ac field will depend, among other things, on the magnitude of the twist elastic constant  $K_2$  of the material. At a  $N-S_A$  transition  $K_2$  diverges so that the temperature behaviour of the optical signal might be quite abrupt as experimentally observed.

Evidently, this treatment of the problem is completely different from the explanations given above. According to this approach, the observed phenomenon is considered as a surface flexoelectric effect of chiral nature rather than a bulk EE.

#### 2.4. Dynamics of the Electroclinic Effect

The study of the relaxational dynamics of the EE in smectics and nematics is based on the assumption that its time dependence is well described by a Debye type equation [1], *i.e.*:

$$\Gamma d\theta/dt + A_S \theta = c \mathbf{E} \quad (9)$$

where  $\Gamma$  is the viscosity relevant to the inclination considered,  $c$  is the electroclinic coupling constant between  $\theta$  and  $\mathbf{E}$ ,  $A_S = a(T - T_o)$  is the so-called tilt controlling susceptibility,  $a$  is a constant,  $T$  is the temperature and  $T_o$  is the transition temperature to a (virtual or existing) tilted phase. This equation neglects all possible interactions of

the molecules with the aligned boundaries. The above approximation will break down in very thin cells as the anchoring interaction with these boundaries gains relative importance over the bulk electroclinic interaction. Van Haaren *et al.* [28] have studied the dependence of the response time on the cell spacing. The main conclusion of their work is that the electroclinic response time increases when the cell thickness becomes very small (about 2  $\mu\text{m}$ ). This dependence has been attributed to a slowing down of the average molecular motion due to the boundaries, which may be described as an increase of the effective viscosity with decreasing cell thickness and decreasing electric field.

If the sample is not thin, it can be deduced from Eq. (9) that a sinusoidal electric field  $\mathbf{E} = E_0 e^{i\omega t}$  of frequency  $\omega$  induces a tilt angle whose amplitude is given by the expression:

$$\theta = (cE_0/A_S)/(1 + \omega^2\tau^2) \quad (10)$$

and the phase delay  $\delta$  of the tilt relative to the field is:

$$\delta = \tan^{-1}(-\omega\Gamma/A_S) = -\tan^{-1}(\omega\tau) \quad (11)$$

where  $\tau = \Gamma/A_S$  is the relaxation time. Then by measuring the phase delay as a function of the frequency, the relaxation time can be determined at each temperature from the slope of a plot of  $\tan \delta$  versus  $\omega$ . These results represent the starting point of the study of the dynamics of the EE. Later, some modifications to this simple theory will be introduced to explain the experimental data.

The dynamics of the electroclinic effect is quite similar in low molecular weight liquid crystals and in polymer liquid crystals. Both kinds of materials follow Eq. (10) reasonably well, at least near the  $S_A - S_C$  transition. The main difference between these two types of liquid crystals is the value of the response time. While response times are in the range of 1–10  $\mu\text{s}$  for low molar mass compounds, under similar conditions, these turn out to be around 1 ms for high molecular weight compounds [12–16]. The reason for this difference is the viscosity coefficient  $\Gamma$ , which is much higher for polymer materials.

### 3. EXPERIMENTAL PROCEDURE

In this section we will describe the experimental set-up for the measurement of the NEE. Special attention will be devoted to some aspects which could hide the phenomenon under test.

#### 3.1. Description of the Measuring Cell

Optical measurements of the NEE are made using the bookshelf geometry. In this configuration, the orientation of the director  $\mathbf{n}$  is parallel to the glass plates containing the liquid crystal. To achieve this orientation, a surfactant such as nylon can be used. It is recommended to cool down the sample very slowly, in order to obtain a good planar sample, without any structural defects. The quality of the alignment is very important for the accuracy of the measurements and must be rigorously examined before any experiment. For the measurement of the NEE it is necessary that the helix in the  $N$  phase must remain unwound a few degrees above the  $N-S_A$  or  $N-S_C$  phase transitions. When the pitch of the helix in the  $N$  phase is larger than the cell spacing, the helix is unwound, so thin cells are suitable.

Electrooptical investigations can be performed by means of the arrangement shown in Figures 4 and 5. The sample, housed in a hot stage, is situated between the crossed polarizers of a polarizing microscope. If the nematic director makes an angle  $\beta$  with the first polarizer and the light intensity is  $I_o$ , the resulting transmitted intensity  $I$  is given by:

$$I = I_o \sin^2 2\beta \sin^2 \phi/2 \quad (12)$$

where  $\phi = 2\pi\Delta n d/\lambda$  is the phase shift through the sample,  $\Delta n$  denotes the birefringence,  $\lambda$  the wavelength of light in vacuum and  $d$  the sample thickness. In the presence of a sinusoidal electric field  $\mathbf{E}$ , a tilt  $\theta$  ( $E$ ) of the optic axis is induced and then the angle between the nematic director and the first polarizer  $\beta(E) = \beta(0) + \theta(E)$  is changed, which provokes a modulation of the light beam  $\delta I$ . In this situation, the tilt angle can be determined monitoring the relative change in the transmitted light intensity:

$$\delta I/I_o = (\sin 4\theta)/\tan 2\beta \quad (13)$$

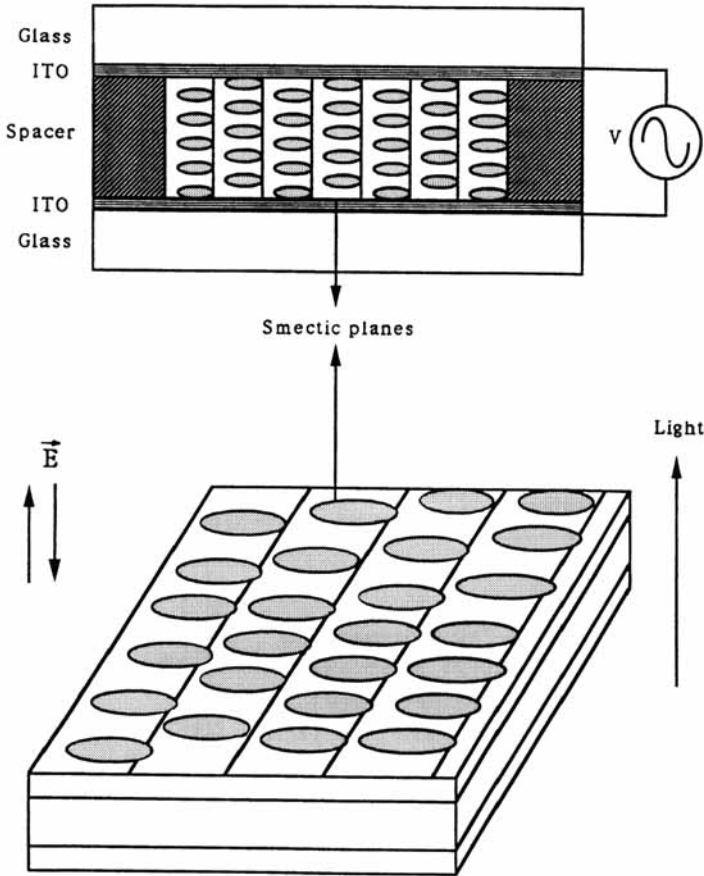


FIGURE 4 Side and top view of the sample cell, showing the geometry used in the experiments.

If the first polarizer makes an angle equal to  $22.5^\circ$  with the nematic director, it follows from the above equation:

$$\theta = \delta I / 4I_0 \tag{14}$$

The modulated light intensity  $\delta I$  is detected with a photodiode and a lock-in amplifier. Simultaneously, the dc intensity  $I_0$  is determined with a digital voltmeter. A tilt out of plane, with a component in the direction of light propagation would produce a light modulation  $\delta I_2$

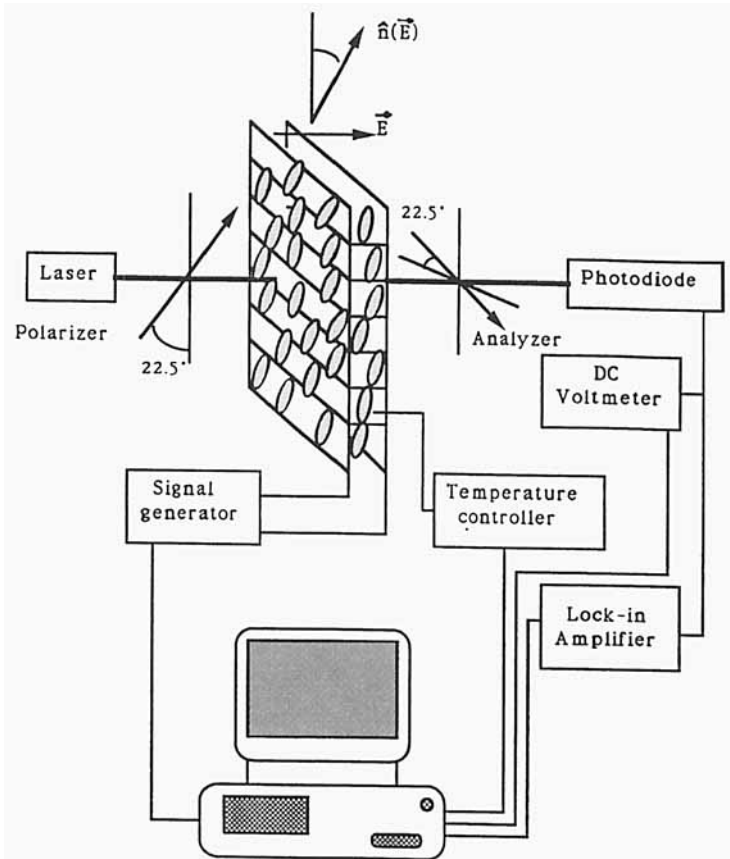


FIGURE 5 Block diagram of the experimental setup used for the optical measurements.

which to lowest order would be proportional to  $\theta^2$  and therefore no signal would be detected at the modulation frequency.

For measurements of the NEE as a function of temperature and field, the driving frequency must be kept fixed at a value of about 1 kHz. This frequency is high enough to prevent the appearance of electrohydrodynamical instabilities in the bulk of the sample which typically develop for frequencies of about 100 Hz or less. It is also lower than the typical relaxation frequency of the NEE.

With this geometry, the above described technique is much more sensitive than the original one with homeotropic alignment proposed

by Garoff *et al.* [1]. Tilt angles as small as  $10^{-7}$  radians can be detected [20].

If the order parameter was spatially varying, there could be a linear coupling between the director and the electric field due to the so-called flexoelectric effect [29]. However, it has been found that the flexoelectric terms are small in the above mentioned geometry [18, 19].

For the relaxation time measurements, the voltage across the sample is kept fixed in the linear response region while the frequency of the signal is varied. Normally, the upper limiting frequency is determined by the lock-in characteristics and can be typically 100 kHz. Special care must be taken with the finite response time of the photodiode and with the relaxational behaviour of the measuring cell. When the relaxation time of the NEE goes down the necessity of taking into account these effects becomes essential. This fact limits the minimum attainable relaxation time to around 50 ns.

Finally, we will indicate that the applied field strength must be high enough to produce a detectable signal and small enough to avoid nonlinear behaviour. In the example shown in Figure 6 it can be deduced that 4 volts is a good trade-off between the above conditions.

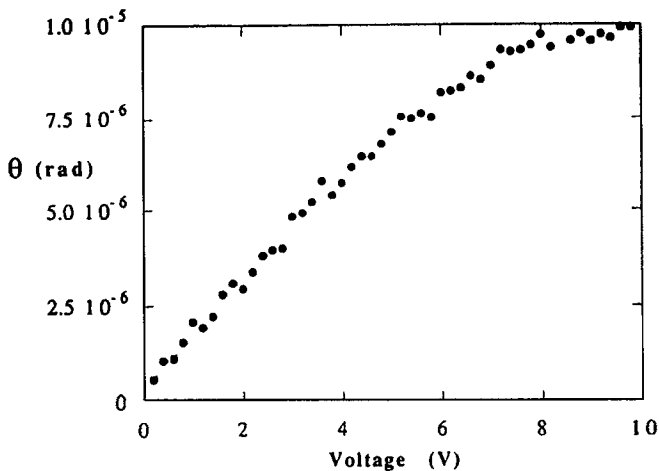


FIGURE 6 Typical results of NEE. A clear deviation from linearity can be observed for voltages above 6 V. Reproduced with permission from Ref. [20].

## 4. RESULTS

Although the NEE was discovered more than five years ago, there are very few reports about this effect. Some of them are basically a brief description of the phenomenon, and others are focused on partial aspects of the effect, such as static or dynamic studies, both from experimental or theoretical points of view. In particular, as far as we know, there is no single report on the NEE in high molecular mass compounds. However, we can expect that this phenomenon can also be detected in polymers. More specifically, we can anticipate the following:

- (a) A similar value of the NEE in the unwound chiral  $N$  phase, than that obtained for low molecular weight compounds.
- (b) A similar behaviour of the induced tilt angle and the response time with temperature. Considering that the viscosity  $\Gamma$  associated to the EE is much higher for polymers, the response time of the NEE should be around one thousand times lower than that corresponding to low molecular weight compounds.

Much of the material presented in this section has already been published in Ref. [30]. However, in view of the lack of examples in the literature it will be repeated here to some extent for the sake of completeness and because it is the most systematic study of the NEE up to now. We will describe the main features of the temperature dependence of the NEE in the  $N$  and  $S_A$  phases for two representative compounds and for the binary mixtures formed with these compounds. We will also present some results of the dynamic behaviour of the NEE. Before beginning to comment the results, the more significant characteristics of these compounds will be given.

### 4.1. Compounds under Test

The materials are two commercial compounds SCE9 and SCE10 from Merck, and binary mixtures made from them. Both compounds are multicomponent mixtures with a large cholesteric pitch over a temperature range several degrees above the nematic–smectic phase transition. The phase transition temperatures as determined by polarizing microscopy are as follows:



329.3	360.4	388.1	
$S_C - S_A - N$	- Isotropic		SCE9
340.1	383.1		
$S_C - N$	- Isotropic		SCE10

Both of them have a negative value of the dielectric anisotropy, so the action of an electric field perpendicular to the molecular director tends to keep it unchanged (there is no Freedericksz transition). This fact makes them suitable for studying the electroclinic response in the  $N$  phase.

The phase diagram of the binary system is shown in Figure 7. The transition temperatures were obtained from measurements of the EE and DSC data. As can be seen, the first order line  $N-S_C$  splits into two  $S_A-S_C$  and  $N-S_A$  lines at the NAC point showing a topology which has been found to be universal [31]. The phase diagram is well

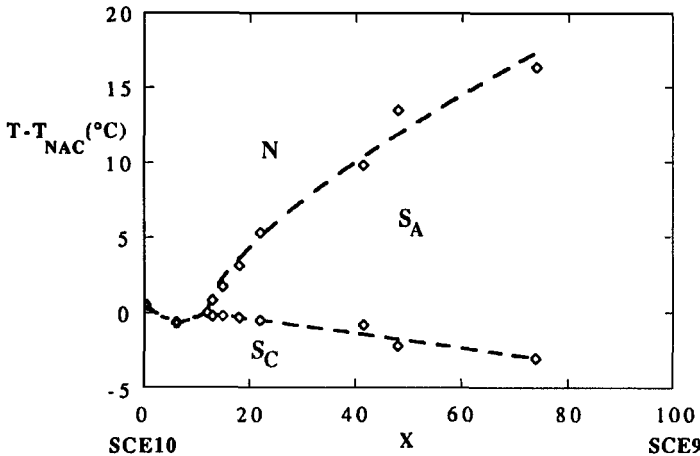


FIGURE 7 Phase diagram of the binary system SCE9 + SCE10.  $X$  represents the wt. percentage of SCE9 in each mixture. Dashed lines are fits to Eq. (15). The parameters corresponding to the best fit are  $\nu = 0.55$ ,  $A_{N-S_A} = 14.72$ ,  $B_{N-S_A} = 9.25$ ,  $A_{S_A-S_C} = -0.155$ ,  $B_{S_A-S_C} = -5.03$ . Redrawn from Ref. [30].

described by the following equations:

$$T_i - T_{\text{NAC}} = A_i(X - X_{\text{NAC}})^\nu + B(X - X_{\text{NAC}}) \quad \text{with} \quad (15)$$

$$i = N - S_C, S_A - S_C, N - S_A$$

where  $T_i$  denotes the temperature of the corresponding transition,  $\nu$ ,  $A_i$  and  $B$  are constants, and  $X$  is the concentration of the compound SCE9. The concentration of the compound SCE9 at the NAC point is  $X_{\text{NAC}} = 0.12 \pm 0.01$  (wt%). All the  $S_A - S_C$  phase transitions are continuous and show a mean-field to tricritical crossover behaviour as the  $S_A$  phase range decreases [32]. The  $N - S_A$  transitions are always second order.

#### 4.2. Study of the Compounds SCE9 and SCE10

Figure 8 shows the temperature dependence of the induced tilt angle  $\theta$  for SCE9. Data were taken over a temperature range from 329.1 K

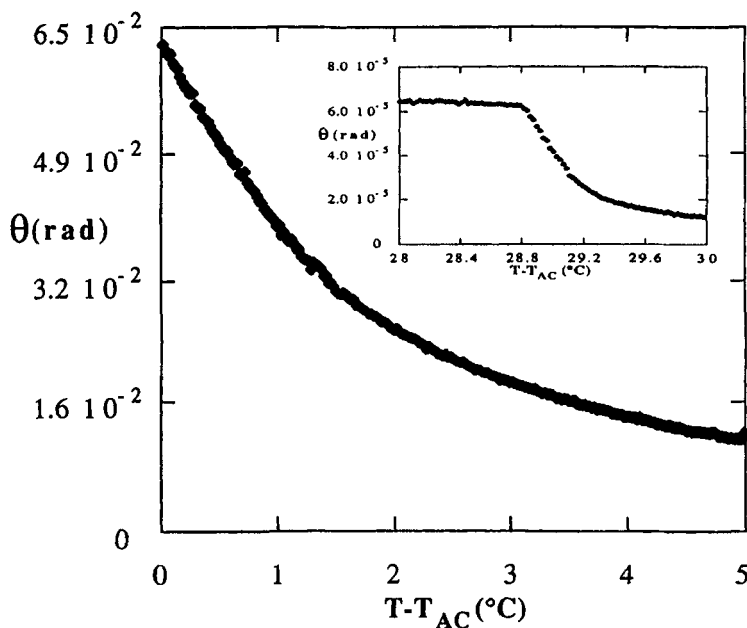


FIGURE 8 Temperature dependence of the tilt angle induced by a sine-wave voltage of 2.5 V and 1 kHz around the phase transitions  $S_A - S_C$  and  $N - S_A$  (inset) of the compound SCE9. The sample thickness was 4  $\mu\text{m}$ . Reproduced with permission from Ref. [30].

(slightly below the  $S_A-S_C$  phase transition) up to 363.1 K (above the  $N-S_A$  phase transition). Within the  $S_A$  phase and near the  $S_A-S_C$  phase transition temperature, the usual pretransitional divergence of the EE is observed. In this region, data can be successfully fitted to a function of the type  $\theta = \theta_0(T-T_{AC})^{-\gamma}$ . The stability of the fit is good and no appreciable dependence of the exponent  $\gamma$  on the number of points taken to fit the results could be noted. The best fit corresponds to a transition temperature  $T_{AC} = 329.3$  K and a susceptibility critical exponent  $\gamma = 1.04 \pm 0.05$  which, according to the expectations, is in good agreement with the predictions of a mean-field model.

Approximately at 360.1 K, the tilt angle drops suddenly down to a small fraction of the value just below the transition. Finally, well inside the  $N$  phase,  $\theta$  is extremely small, showing a monotonous decreasing tendency with increasing temperature. It is shown in the figure that the values of the tilt angle in the  $N$  and  $S_A$  phases are quite different. Obviously, the coupling between the tilt angle and the molecular polarization is influenced by the degree of order in the liquid crystalline phase, so a big increase at the transition from a  $N$  phase to a more ordered  $S_A$  phase is not striking. This feature has been also observed in the transitions between smectic nontilted phases with different in-plane order [11].

According to the model proposed in [19], the induced tilt in the  $N$  phase should be proportional (except for an additive constant) to the square of the smectic order parameter  $|\psi|^2$ . Therefore  $\theta$  must have a temperature dependence given by the renormalization-group expression:

$$\theta = \theta_0 + G|t|^\alpha + H|t| \quad (16)$$

where  $\alpha$  is the critical exponent for the specific heat,  $G$  and  $H$  are constants,  $t = (T-T_{NA})/T_{NA}$  is the reduced temperature and  $\theta_0$  the tilt at  $T_{NA}$ . However, Eq.(16) fails to account properly for the experimental results [20]. Although the resulting fits are not bad, no convergence for the parameters can be achieved as stability of the fits is tested by range shrinking. Furthermore, the variation for the critical exponent  $\alpha$  deduced from the fits is completely unrealistic.

In Figure 9 we have plotted the temperature dependence of the induced tilt angle in the  $N$  phase of SCE10. As can be seen,  $\theta$  changes very little over a broad range in the  $N$  phase and then grows suddenly

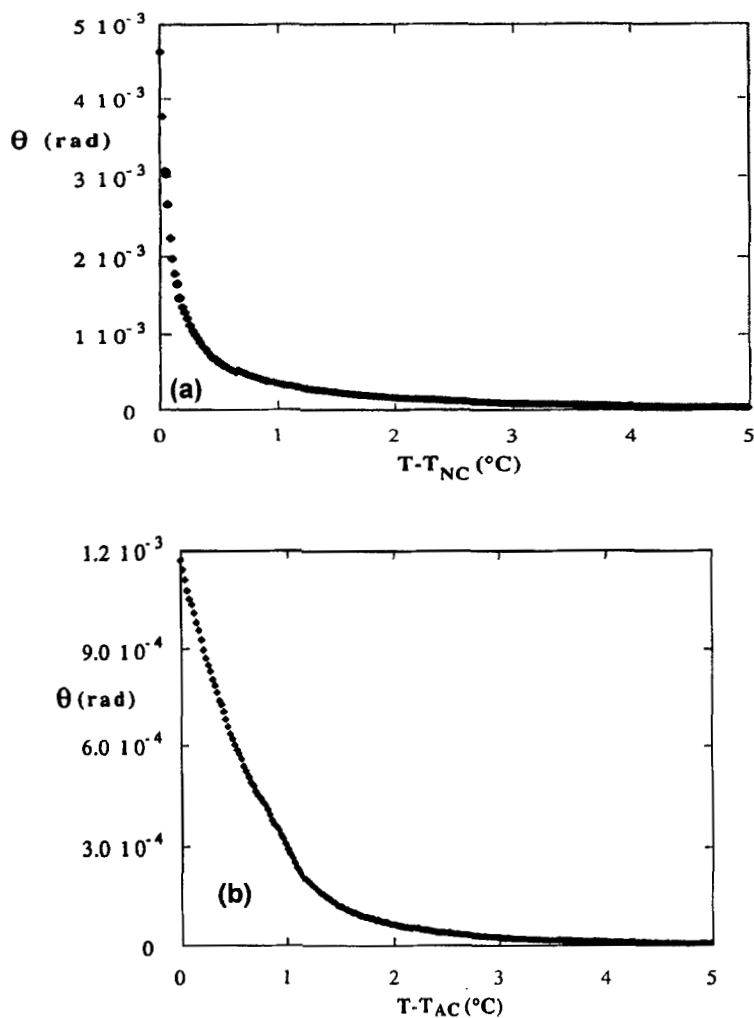


FIGURE 9 Evolution of the molecular tilt angle with temperature for the compound SCE10 around the  $N$ - $S_C$  phase transition. For this measurement a sine-wave voltage of 2.5 V and 1 kHz was applied to a sample of  $4 \mu\text{m}$ . Reproduced with permission from Ref. [30].

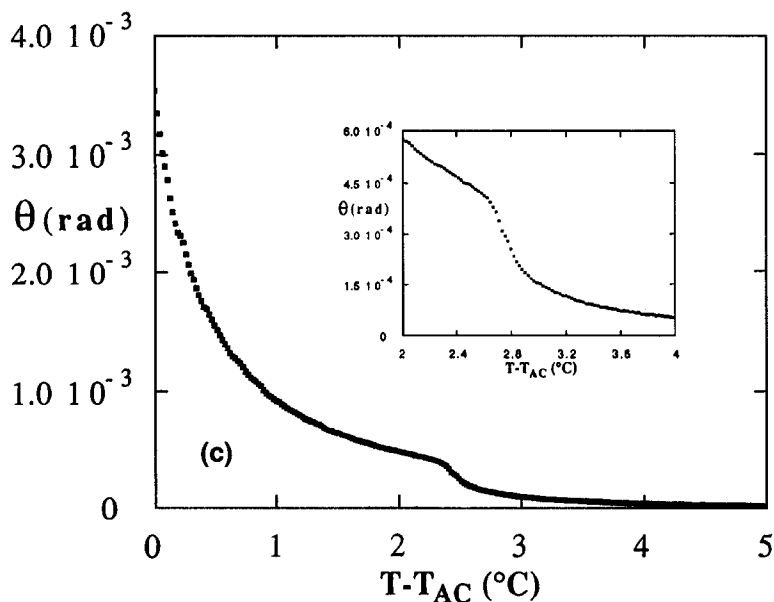


FIGURE 9 (Continued).

in the proximity of the  $N-S_C$  transition temperature  $T_{NC}$ . The induced tilt angle in the  $N$  phase of this compound is much higher than that of SCE9, with a  $N-S_A$  phase transition. This is in qualitative agreement with the behaviour of the NEE estimated from dielectric measurements in a short-pitch cholesteric material [33], although the numerical values reported in that work are much larger than those presented here and in other studies using optical techniques [18–20, 30]. In any case, an increase of the NEE near a  $N-S_C$  transition is what can be expected from the diverging coherence length of the  $S_C$  fluctuations at  $T_{NC}$ .

### 4.3. Study of Binary Mixtures

In the last section we have described separately the most relevant features of the EE in the  $N$  phase of the compounds SCE9 and SCE10. In order to get a better understanding about the effect of the phase

sequence on the magnitude and evolution of the NEE, we will now describe the induced tilt angle behaviour in the  $N$  phases of mixtures made from SCE9 and SCE10.

Figure 10 shows the temperature dependence of the NEE for several mixtures. It can be seen that, as a general trend, when the range of the  $S_A$  phase is reduced, the magnitude of the NEE increases. In contrast, the opposite evolution is displayed by the induced tilt close to  $T_{AC}$ .

One way to characterize the behaviour and size of the NEE for the different mixtures is by means of the value and the slope of  $\theta$  at  $T_{NA}$ . Table I shows these quantities for all mixtures. For the mixtures close to the NAC point, both the NEE and its derivative are much greater than those that possess a broad  $S_A$  range. In fact, for mixture ( $X = 13$ ), with only one degree of  $S_A$  phase, the only noticeable effect of the transition  $N-S_A$  is a slight modification of the shape of the curve, around this position. In this case and at a first glance the EE behaves as if it was due to a unique continuous process, identical in both the  $N$  and  $S_A$  phases and smoothly altered by the  $N-S_A$  phase transition. Similar results have been obtained by Legrand *et al.*, using dielectric spectroscopy [33].

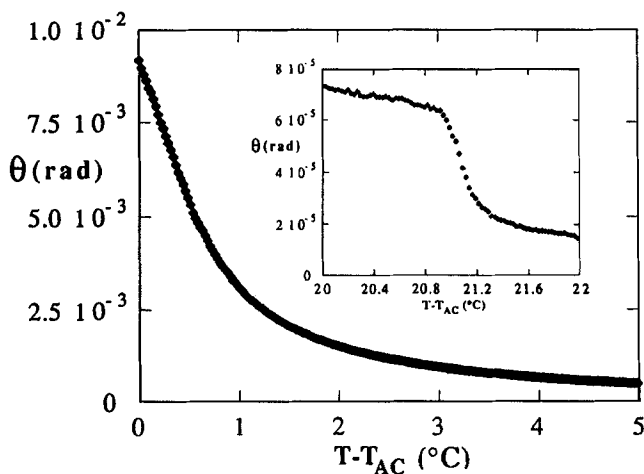


FIGURE 10 Temperature dependence of the induced tilt angle for several mixtures around the  $N-S_A$  transition. The wt. percentage of SCE9 and the temperature range of the  $S_A$  phase are the following: (a)  $X = 13$ ;  $T_{NA} - T_{AC} = 1.0^\circ\text{C}$ , (b)  $X = 18$ ;  $T_{NA} - T_{AC} = 2.8^\circ\text{C}$ , (c)  $X = 75$ ;  $T_{NA} - T_{AC} = 21^\circ\text{C}$ . Reproduced with permission from Ref. [30].

TABLE I Magnitude and slope of the induced tilt  $\theta$  at the  $N-S_A$  transition temperature  $T_{NA}$  as a function of the  $S_A$  range.  $X$  represents wt. percentage of SCE9 in each SCE9 + SCE10 mixture. For pure SCE10 ( $X = 0$ ) we have written the values of  $\theta$  and its derivative at the  $N-S_C$  transition temperature. In all cases, the applied field amplitude was  $2.5 \text{ V}/4 \mu\text{m}$

$X/\text{percent}$	$S_A \text{ range}/K$	$\theta(T_{NA})/\text{rad}$	$(d\theta/dT)(T_{NA})/\text{rad } K^{-1}$
0	0	$4.01 \cdot 10^{-3}$	$2.10 \cdot 10^{-2}$
13	1	$2.53 \cdot 10^{-4}$	$7.10 \cdot 10^{-4}$
15.4	1.9	$2.99 \cdot 10^{-4}$	$6.11 \cdot 10^{-4}$
18	2.8	$2.81 \cdot 10^{-4}$	$5.00 \cdot 10^{-4}$
22	3.8	$2.69 \cdot 10^{-4}$	$3.47 \cdot 10^{-4}$
75	21	$4.16 \cdot 10^{-5}$	$1.71 \cdot 10^{-4}$
100	29	$3.05 \cdot 10^{-5}$	$1.60 \cdot 10^{-4}$

Moreover, the amplitude of the induced tilt angle at  $T_{NA}$  is not linear with the concentration of SCE10. It is observed a systematic trend to a diverging behaviour from the values of the slopes as the concentration of SCE10 increases. As reported by Marcerou [26], a diverging behaviour is to be expected at the NAC multicritical point.

As before, any attempt to fit the curves  $\theta(T)$  in the  $N$  phase to Eq. (16) becomes unsuccessful when the validity of these fits is checked by range shrinking.

#### 4.4. Dynamics of the NEE in SCE9

Figure 11 represents the tangent of the phase  $\delta$  versus frequency for three chosen temperatures in the  $S_A$  phase. The relaxation time is directly determined from the slope of these plots. As can be seen, the expected linear relationship between  $\tan \delta$  and  $\omega$  (Eq. (12)) is reasonably well followed, although some small deviations from this behaviour appear at low temperatures. Nevertheless, the variations of the slope are small enough to assume, that at least, in the frequency range  $10^3 - 10^5 \text{ Hz}$  only one important mechanism is involved. The relaxation times obtained from the linear fits are shown in Figure 12. At low temperatures in the  $S_A$  phase,  $\tau$  presents the usual diverging behaviour which corresponds to the soft mode evolution. However, on approaching the  $N-S_A$  transition from below an unexpected increase of the relaxation time is observed, very similar to that reported by Li *et al.* [34]. Finally, above the  $N-S_A$  phase transition, the relaxation time is a monotonically decreasing function of temperature with a sharp slope

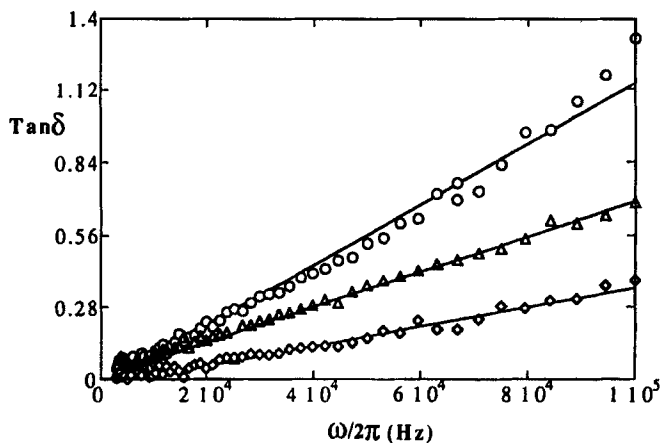


FIGURE 11 Tangent of the phase angle  $\delta$  between the induced tilt angle and the applied field as a function of frequency at several temperatures in the  $S_A$  phase of the compound SCE9. The applied field was  $2.5 \text{ V}/4 \mu\text{m}$ . Continuous lines represent the best fits to straight lines. Reproduced with permission from Ref. [30].

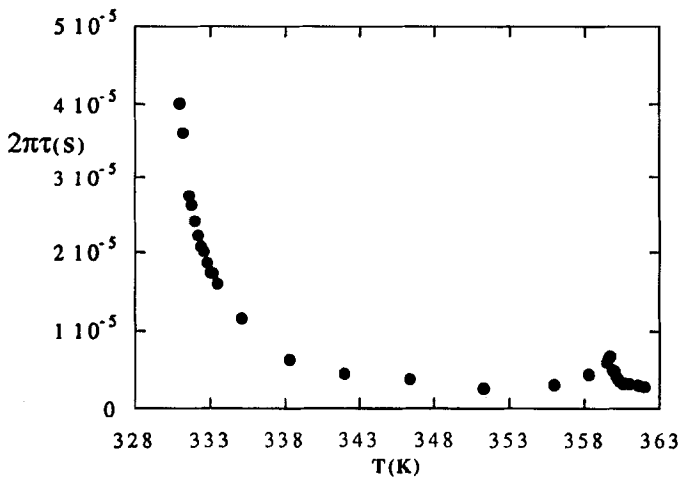


FIGURE 12 Response time  $\tau$  of the electroclinic effect versus temperature for the compound SCE9. The anomalous behaviour at the  $N-S_A$  transition is clearly visible. Reproduced with permission from Ref. [30].

near  $T_{NA}$ . This behaviour has similar features to those found in Ref. [33], although in that work no peak at the  $N-S_A$  transition could be observed.



## 5. DISCUSSION

This last section will be dedicated to discuss the above results in view of the theories have appeared to explain the NEE. First of all, we will show that NEE is mainly driven by a bulk process. Then, we will deal more specifically with some bulk mechanisms, which, to some extent, seem to be responsible of the NEE. The results on the NEE dynamics will give us some insight about the relative importance of the different contributions which intervene in this effect.

### 5.1. Surface Nature *versus* Bulk Nature of the NEE

As has been pointed out above, one possible explanation for the NEE is to consider the phenomenon as a surface flexoelectric effect of chiral nature rather than an actual bulk EE [27]. In the presence of an electric field the surface molecules would tilt respect to the rubbing axis and the rotation of the alignment at the surface would be transmitted to the whole sample thickness *via* the twist elastic constant  $K_2$ .

Nevertheless, there exists a serious drawback in considering the NEE as a surface effect. The problem is the order of magnitude of the response time predicted by the model, which is not consistent with that experimentally observed. If the NEE was driven by an interfacial mechanism, the response time  $\tau$  would be expected [25] to be of the order of  $\tau = \eta d^2 / \pi^2 K_2$ . Taking a typical viscosity  $\eta = 0.1$  P and  $K_2 = 10^{-11}$  N,  $\tau$  results to be in the range  $10^{-2} - 10^{-3}$  s for a  $d = 4$   $\mu$ m sample. As has been shown before (Fig. 12), this is three or four orders of magnitude greater than the measured times. Moreover, this explanation predicts a dependence of the relaxation time on the square of the sample thickness which has not been observed [35]. It is worth pointing out however, that recently a surface-mediated NEE has been in fact observed in homeotropic cells [36], so this new phenomenon actually does exist as expected from the above argument. The effect presents relaxation times as high as  $10^{-2}$  s and its size is much larger than what we have observed. However, given the frequency range used in the NEE measurements and the magnitude of the induced tilt, the contribution from this interfacial process is expected to be negligible.

Another possible surface mediated origin of the NEE is the existence of smecticlike order close to the surface [37]. These surface smectic layers can be formed by the action of the polar interaction between the chiral liquid crystal and the bounding plates. In these sample regions, molecules would be tilted when an electric field is applied to the sample. The inclination of the molecules at the surface would be transmitted to the bulk of the sample *via* elastic interactions. In this way, the rapid change in magnitude of the induced tilt could be understood in terms of the variations of the surface smectic order, which has a strong temperature dependence. In this hypothesis, the EE would be proportional to the smectic order parameter  $|\Psi|^2$ . An in-plane electric field could then couple to the molecular dipole and induce a tilt at the surface. For electric fields of sufficiently low frequency, the surface tilt propagates elastically inside the sample and gives rise to an observable bulk deformation with an average tilt angle:

$$\theta = l^{-1} \int \theta(z) dz \quad (17)$$

where  $l$  is a temperature dependent penetration length, characteristic of the surface layer. However, as before, the relaxation times should be lower than those actually observed. In this situation we can conclude that the NEE is mainly driven by a bulk mechanism.

## 5.2. Cybotactic Clusters or Molecular Origin

As has been pointed out in Section 2, when dealing with the EE we must distinguish between the effect in orthogonal smectic mesophases and the effect in chiral phases without layers, such as the  $N$  or even isotropic phases [35]. In smectic phases, the layer normal provides a reference direction that permits one to distinguish energetically between untilted and tilted configurations. This allows the molecules to tilt physically when an electric field is applied. As a consequence of this mechanism, the smectic layers are forced to lower their thickness and, in order to avoid this contraction (quite unfavourable from the energetic point of view), the planes should deform. The actual existence of this physical tilt in the conventional EE has been indirectly observed by some authors, who have proposed an undulation of the

planes [38] or the bending or tilting of the layer structure [39] when an electric field is applied.

In contrast, in the case of  $N$  phases, this mechanism is, in principle, not allowed if the NEE is assumed to be a bulk effect. The only possibility to impose locally a preferred axis in an  $N$  phase is to include the presence of smectic cybotactic groups (Fig. 3). Since, on average, the molecular director in these groups is parallel to the director in the  $N$  phase, the process responsible for the EE in smectics could also operate for the NEE.

On the other hand, it is clear that the NEE can also appear as an inclination of the optical indicatrix without any tilt of the usual nematic director ( $\mathbf{n}_1$  in Fig. 2). Although this process does not produce a net restoring torque linear in the electric field, there is no reason that prevents this contribution from working also in smectic phases. However, presumably, this mechanism is much less efficient than the former one and, given the small value of the NEE, it is expected to be negligible in phases with translational order.

Having stated these ideas, we begin comparing the results obtained for the compounds SCE9 and SCE10. Although the chemical structure of these materials is unknown to us, it seems reasonable to assign similar values to the molecular transverse dipole moment, since the spontaneous polarization in the corresponding  $S_C$  phases is similar in both cases (about  $25 \text{ nCcm}^{-2}$  at room temperature). Therefore, the strong difference exhibited by the induced tilt can only be related with the kind of phase sequence. Since the effect is two orders of magnitude higher in SCE10, with a  $S_C$  phase below the  $N$  phase, it seems likely that the  $S_C$  fluctuations play an important role in the explanation of the phenomenon [26, 33]. Moreover, in compounds with a transition sequence  $N-S_C$ , the coupling between the smectic order parameter  $|\Psi|$  and the tilt angle  $\theta$  is very strong. This idea is supported by the behaviour displayed by the SCE9 + SCE10 mixtures, which show an increasing magnitude of the tilt and its derivative as the  $S_A$  range is reduced and the tilted smectic fluctuations become more important.

It can be argued that this increasing effect is reasonable because the induced tilt in the  $S_A$  phase must also grow, due to its proximity to a  $S_C$  phase, where the tilt susceptibility diverges. In addition, as has been pointed out above, the hypothesis of proportionality between  $\theta$  and  $|\Psi|^2$  may fail if the  $N-S_A$  transition is close to a  $S_A-S_C$  transition.

Nevertheless, we can also notice that for mixtures close to the NAC multicritical point, the EE appears as if it was driven by a single process both in the  $N$  and  $S_A$  phases. Thus, this seems to suggest a unique main mechanism for the induced tilt in both phases. Furthermore, if the contribution of the smectic cybotactic domains is relevant in the explanation of the NEE, it is not clear that the induced tilt should be well approximated simply by a term proportional to  $|\Psi|^2$ . In this approach, the problem becomes more complicated. Only one part of the induced tilt would behave like  $|\Psi|^2$ . It is therefore not surprising that Eq. (16) cannot account properly for the results obtained. An expression for the other contributions would involve material quantities such as correlation lengths of the smectic domains and the elastic constants of the  $N$  phase with no simple prediction for the apparent critical exponent [26]. All these ideas can be summarized schematically by the following equation:

$$\theta(T) = \theta_{nc}(V - V_c)/V + \theta_c V_c/V \quad (18)$$

where  $V$  is the volume of the liquid crystal,  $\theta_c$  is the contribution of the cybotactic groups, which depends, among other things, on the kind of nematic–smectic transition;  $V_c$  is the total volume of the cybotactic groups, which is strongly temperature dependent and  $\theta_{nc}$  represents the non cybotactic contribution, which as we have said before, behaves as  $|\Psi|^2$ . Very close to the nematic–smectic transition, and for materials with a small  $S_A$  range, not only  $\theta_c$  but also  $V_c$  are large, so this term will be the most important. On the other hand, not very close to the transition or for compounds with large  $S_A$  phases, the first term would be the main one.

In principle, we consider that both mechanisms could give rise to the observed anomalous behaviour of the NEE. In any case it seems clear that the NEE depends strongly on the degree of smectic order. The flexibility between the dipole moment and the optical core is reduced in the smectic state, so bent conformations of the molecules are less probable in phases with translational order. This fact should contribute to improve the efficiency of the coupling between the dipole moment and the electric field.

### 5.3. Dynamics of the NEE

At this point it is interesting to discuss the temperature dependence of  $\tau$  both in the  $S_A$  and  $N$  phases. Near  $T_{AC}$ ,  $\tau$  increases abruptly as we approach the  $S_C$  phase. This behaviour is classical and corresponds to the critical slowing down of the mode whose softening gives rise to the  $S_C$  phase. Similar behaviour is observed in the dielectric response [23]. However, at the  $S_A$  side, near the  $N-S_A$  transition,  $\tau$  increases again with increasing temperature. As has been pointed out before, the temperature dependence is similar to that found by Li *et al.* [34] and differs considerably from the behaviour predicted by the available theoretical models. Above the  $N-S_A$  transition,  $\tau$  decreases again, and at temperatures well inside the  $N$  phase the effect is so small and fast that reliable measurements become problematic. In the case of material with the  $N-S_C$  transition, preliminary results indicate a similar tendency for the temperature dependence of the response time at the  $N$  side [35].

It is difficult to explain the obtained results around the  $N-S_A$  point, especially those at the  $S_A$  side. Given our current understanding of the EE and since there is apparently only one relaxation mechanism,  $\tau$  should be proportional to the induced tilt angle both in the  $S_A$  and  $N$  phases. In [34], the cusplike anomalous slowing down of  $\tau$  in the  $S_A$  phase has been explained in terms of two relaxation mechanisms whose contributions to the tilt susceptibility subtract, thus giving an effective time larger than either of the two individual processes. In the referred work, these two relaxations are associated to the “in-phase” and “out-of-phase” amplitude fluctuations in the tilt and polarization as described in [40]. However, several difficulties arise when comparing the experimental data and the predictions of this model. First, unless the two relaxation frequencies have quite similar values, the deviation of the effective  $\tau$  from the relaxation time of the slower process is negligible. Furthermore, if the temperature dependence of the characteristic times of the two modes follows the classical predictions it is difficult to reproduce the sharp experimental behaviour near  $T_{NA}$ . Finally, the fact that a similar anomaly has been found at least in two compounds near a  $N$  phase suggests that the existence of the  $N-S_A$  transition must presumably be involved in the effect.

Another scheme for the NEE, which at least, is able to connect the anomaly of  $\tau$  with the presence of the  $N-S_A$  transition can be

proposed. In the line of the above reasoning, one could think of the biasing of the rotation of the molecules around their long axes as one fast mechanism competing simultaneously with the physical tilt of the molecules (tilt of the nematic director) in the  $S_A$  phase. The last contribution would be driven by the usual process which softens at the  $S_A-S_C$  transition. On the other hand, the fast process would be associated with the rotational motion around the molecular long axis. Well inside the  $N$  phase only this fast process would operate. However, in order to explain the shape of the observed  $\tau$  curve it is necessary that the contributions to the tilt susceptibility of both mechanisms are of similar size or their characteristic frequencies become of the same order of magnitude in this region. If this model is correct, the anomaly of  $\tau$  at the  $N-S_A$  transition could have a different shape in other materials. This would occur if the contributions of both processes to the tilt susceptibility add instead of subtract. However, dielectric measurements of this compound do not seem to support these ideas [23]. Although, two different modes have been found, the relaxation frequencies are very different.

Another possibility to explain the dynamics of the NEE can still be constructed. Some authors have found an indication of the bending of the layer structure in the smectic phase due to the layer shrinking associated to the molecular tilt. The dynamic response observed by these authors can be decomposed into at least two components with time constants about 0.7 and 3  $\mu\text{s}$  [39]. The fast process is associated with the director switching while the other one is connected to the layer structure change. As the relaxation times of these different processes are similar the anomalous behaviour of the EE near the  $N-S_A$  transition could be explained. However other authors have found that the undulation of the smectic layer is characterized by a relaxation frequency which is two orders of magnitude lower the relaxation frequency of the soft mode. If this is correct, the difference in frequencies for the two intervening processes again forces us to discard this hypothesis [38].

## 6. CONCLUSIONS

In conclusion, we have analyzed the origin of the NEE. Results of the induced tilt magnitude as a function of the temperature range of the

subsequent  $S_A$  phase suggest that short range smectic fluctuations can play an important role in the NEE at least when a  $S_C$  phase is close to the nematic. On the other hand from the dynamical behaviour of the NEE we have deduced that the NEE is mainly driven by bulk processes. Therefore, the biasing of the molecular rotation by the field seems to be the principal cause of the NEE, although the anomaly of  $\tau$  around the transition indicates the existence of, at least, another competing mechanism.

### Acknowledgements

This work is supported by the CICYT of Spain (project MAT94-0717-C02-02) and the EC Human Capital and Mobility Programme (project ERB-4050-PL922749).

### References

- [1] Garoff, S. and Meyer, R. B. (1977). *Phys. Rev. Lett.*, **38**, 848.
- [2] Meyer, R. B., Liebert, L., Strzelecki, L. and Keller, P. (1975). *J. Physique Lett.*, **36**, L. 69.
- [3] Andersson, G., Dahl, I., Keller, P., Kuczynski, W., Lagerwall, S. T., Skarp, K. and Stebler, B. (1987). *Appl. Phys. Lett.*, **51**, 640.
- [4] Bahr, Ch. and Heppke, G. (1987). *Liq. Cryst.*, **2**, 825.
- [5] Nishiyama, S., Ouchi, Y., Takezoe, H. and Fukuda, A. (1987). *Jpn. J. Appl. Phys.*, **26**, L1787.
- [6] Qiu, R., Ho, J. T. and Hark, S. K. (1988). *Phys. Rev. A*, **38**, 1653.
- [7] Li, Z. and Rosenblatt, C. (1989). *Phys. Rev. A*, **39**, 1594.
- [8] Etxebarria, J., Remón, A., Tello, M. J. and Serrano, J. L. (1989). *Liq. Cryst.*, **4**, 543.
- [9] Andersson, G., Dahl, I., Kuczynski, W., Lagerwall, S. T., Skarp, K. and Stebler, B. (1988). *Ferroelectrics*, **84**, 285.
- [10] Andersson, G., Dahl, I., Komitov, L., Lagerwall, S. T., Skarp, K. and Stebler, B. (1989). *J. Appl. Phys.*, **66**, 4983.
- [11] Bahr, Ch. and Heppke, G. (1988). *Phys. Rev. A*, **37**, 3179.
- [12] Verrall, M., Coates, D. and Sage, I. (1996). *Ferroelectrics*, **181**, 241.
- [13] Beer, A., Scherowsky, G. and Wolff, D. (1996). *Ferroelectrics*, **181**, 249.
- [14] Moritake, H., Fuwa, Y., Sagioka, K., Watanabe, T., Ozaki, M., Yoshino, K. and Hwang, J. C. (1996). *Ferroelectrics*, **181**, 307.
- [15] Svensson, M., Helgee, B., Skarp, K., Andersson, G. and Hermann, D. (1996). *Ferroelectrics*, **181**, 319.
- [16] Verrall, M., Beattie, D., Coates, D., Sage, I. and Lymer, K. (1996). *Ferroelectrics*, **181**, 327.
- [17] Komitov, L. (1991). Invited Lecture at the Second International Meeting on Optics of Liquid Crystals, Torino (Italy), 1988; Komitov, L., Lagerwall, S. T., Stebler, B., Andersson, G. and Flatishler, K., *Ferroelectrics*, **114**, 169.
- [18] Li, Z., Petschek, R. G. and Rosenblatt, C. (1989). *Phys. Rev. Lett.*, **62**, 769 (1989); **62**, 1577(E).

- [19] Li, Z., Lisi, A. D., Petschek, R. G. and Rosenblatt, C. (1990). *Phys. Rev. A*, **41**, 1997.
- [20] Etxebarria, J. and Zubia, J. (1991). *Phys. Rev. A*, **44**, 6626.
- [21] Li, Z., Ambigapathi, R., Petschek, R. G. and Rosenblatt, C. (1991). *Phys. Rev. A*, **43**, 7109.
- [22] Garoff, S. and Meyer, R. B. (1979). *Phys. Rev. A*, **198**, 338.
- [23] Zubia, J., Ezcurra, A., de la Fuente, M. R. and Pérez Jubindo, M. A. (1991). *Liq. Cryst.*, **10**, 849.
- [24] Williams, P. A., Clark, N. A., Ros, M. B., Walba, D. M. and Wand, M. D. (1991). *Ferroelectrics*, **121**, 143.
- [25] de Gennes, P. G., "The Physics of Liquid Crystals", pp. 74–76 (Clarendon, Oxford 1974).
- [26] Marcerou, J. P. (1994). *J. Phys. II France*, **4**, 751.
- [27] Dahl, I. (1990). "On Order, Ferroelectricity and Elasticity in Smectic Liquid Crystals", *Ph.D. Thesis*, Göteborg.
- [28] van Haaren, J. A. M. M. and Rikken, G. L. J. A. (1989). *Phys. Rev. A*, **40**, 5476.
- [29] Meyer, R. B. (1969). *Phys. Rev. Lett.*, **22**, 918.
- [30] Zubia, J., Etxebarria, J. and Pérez Jubindo, M. A. (1994). *Liq. Cryst.*, **16**, 941.
- [31] Martínez Miranda, L. T., Kortan, A. R. and Birgeneau, R. G. (1987). *Phys. Rev. A*, **36**, 2372.
- [32] Zubia, J., Castro, M., Puértolas, J. A., Etxebarria, J., Pérez Jubindo, M. A. and de la Fuente, M. R. (1993). *Phys. Rev. E*, **48**, 2749.
- [33] Legrand, C., Isaert, N., Hmine, J., Buisine, J., Parneix, J. P., Nguyen, H. T. and Destradé, C. (1992). *J. Phys. France II*, **2**, 1545.
- [34] Li, Z., Atkins, R. B., Dilisi, G. A., Rosenblatt, C. and Petschek, R. G. (1991). *Phys. Rev. A*, **43**, 852.
- [35] Zubia, J. (unpublished results).
- [36] Chandrall, K. A., Trapathi, S. and Rosenblatt, C. (1992). *Phys. Rev. A*, **46**, R715.
- [37] Lee, S. D. and Patel, J. S. (1991). *Phys. Rev. A*, **44**, 2749.
- [38] Pavel, J. and Glogarova, G. (1991). *Ferroelectrics*, **114**, 113.
- [39] Johno, M., Chandani, D. L., Takanishi, Y., Ouchi, Y., Takezoe, H. and Fukuda, A. (1991). *Ferroelectrics*, **114**, 123.
- [40] Blinc, R. and Zeks, B. (1978). *Phys. Rev. A*, **18**, 740.